

## RESEARCH ARTICLE

10.1002/2015JG003025

## Key Points:

- Two-year eddy covariance measurements of large-lake latent, sensible heat, and CO<sub>2</sub> fluxes
- Western Lake Erie acted as a yearly CO<sub>2</sub> source but a small CO<sub>2</sub> sink in summers
- Western Lake Erie returns approximately 90% of annual rainfall via evaporation

## Supporting Information:

- Supporting Information S1

## Correspondence to:

C. Shao,  
clshao@msu.edu

## Citation:

Shao, C., J. Chen, C. A. Stepien, H. Chu, Z. Ouyang, T. B. Bridgeman, K. P. Czajkowski, R. H. Becker, and R. John (2015), Diurnal to annual changes in latent, sensible heat, and CO<sub>2</sub> fluxes over a Laurentian Great Lake: A case study in Western Lake Erie, *J. Geophys. Res. Biogeosci.*, 120, 1587–1604, doi:10.1002/2015JG003025.

Received 19 APR 2015

Accepted 16 JUL 2015

Accepted article online 20 JUL 2015

Published online 14 AUG 2015

## Diurnal to annual changes in latent, sensible heat, and CO<sub>2</sub> fluxes over a Laurentian Great Lake: A case study in Western Lake Erie

Changliang Shao<sup>1</sup>, Jiquan Chen<sup>1</sup>, Carol A. Stepien<sup>2</sup>, Housen Chu<sup>3</sup>, Zutao Ouyang<sup>1</sup>, Thomas B. Bridgeman<sup>2</sup>, Kevin P. Czajkowski<sup>2</sup>, Richard H. Becker<sup>2</sup>, and Ranjeet John<sup>1</sup>

<sup>1</sup>Center for Global Change and Earth Observations, Michigan State University, East Lansing, Michigan, USA, <sup>2</sup>Lake Erie Center, University of Toledo, Oregon, Ohio, USA, <sup>3</sup>Department of Environmental Science, Policy, and Management, University of California, Berkeley, California, USA

**Abstract** To understand the carbon and energy exchange between the lake surface and the atmosphere, direct measurements of latent, sensible heat, and CO<sub>2</sub> fluxes were taken using the eddy covariance (EC) technique in Western Lake Erie during October 2011 to September 2013. We found that the latent heat flux (*LE*) had a marked one-peak seasonal change in both years that differed from the diurnal course and lacked a sinusoidal dynamic common in terrestrial ecosystems. Daily mean *LE* was  $4.8 \pm 0.1$  and  $4.3 \pm 0.2$  MJ m<sup>-2</sup> d<sup>-1</sup> in Year 1 and Year 2, respectively. The sensible heat flux (*H*) remained much lower than the *LE*, with a daily mean of  $0.9 \pm 0.1$  and  $1.1 \pm 0.1$  MJ m<sup>-2</sup> d<sup>-1</sup> in Year 1 and Year 2, respectively. As a result, the Bowen ratio was <1 during most of the 2 year period, with the lowest summer value at 0.14. The vapor pressure deficit explained 35% of the variation in half hourly *LE*, while the temperature difference between the water surface and air explained 65% of the variation in half hourly *H*. Western Lake Erie acted as a small carbon sink holding  $-19.0 \pm 5.4$  and  $-40.2 \pm 13.3$  g C m<sup>-2</sup> in the first and second summers (May–September) but as an annual source of  $77.7 \pm 18.6$  and  $49.5 \pm 17.9$  g C m<sup>-2</sup> yr<sup>-1</sup> in Year 1 and Year 2, respectively. The CO<sub>2</sub> flux (*F*<sub>CO<sub>2</sub></sub>) rate varied from  $-0.45$  g C m<sup>-2</sup> d<sup>-1</sup> to  $0.98$  g C m<sup>-2</sup> d<sup>-1</sup>. Similar to *LE*, *F*<sub>CO<sub>2</sub></sub> had noticeable diurnal changes during the months that had high chlorophyll *a* months but not during other months. A significantly negative correlation (*P* < 0.05) was found between *F*<sub>CO<sub>2</sub></sub> and chlorophyll *a* on monthly fluxes. Three gap-filling methods, including marginal distribution sampling, mean diurnal variation, and monthly mean, were quantitatively assessed, yielding an uncertainty of 4%, 6%, and 10% in *LE*, *H*, and *F*<sub>CO<sub>2</sub></sub>, respectively.

### 1. Introduction

Lakes play important roles in determining local, regional, and even global climate through complex interactions of biophysical and biogeochemical processes [Rouse *et al.*, 2005; Cole *et al.*, 2007; Nordbo *et al.*, 2011]. The Laurentian Great Lakes contain 20% of the Earth's surface freshwater and are highly influential on water and carbon budgets in the North America. As the largest inland water ecosystem, the albedo, heat capacity, roughness, surface evaporation, and greenhouse gas exchange of the Great Lakes differ greatly from those in the surrounding landscapes [O'Donnell *et al.*, 2010]. Understanding these exchanges and the environmental controls over this open water surface is therefore critical when quantifying the influences on the regional climate and weather [Vesala *et al.*, 2006; Liu *et al.*, 2009; Polensaeere *et al.*, 2013]. Yet the changes of carbon and water fluxes over the lake surfaces have not been reported, especially at broader temporal scales (monthly, seasonal, and yearly), due to the difficulties in collecting reliable observations over the open water [Atilla *et al.*, 2011; Bennington *et al.*, 2012].

Previous studies reported that inland lakes have significant impacts on local/regional water and energy cycles [Eugster *et al.*, 2003; Long *et al.*, 2007; Liu *et al.*, 2012]. Globally, lake evaporation (*E*) is an important atmospheric moisture source that returns ~60% of annual lake precipitation to the atmosphere [Oki and Kanae, 2006], affecting water resources, climate, and vegetation at multiple spatial-temporal scales [Blanken *et al.*, 2000; Xiao *et al.*, 2013]. Accurate information on the exchanges of energy and water between the lake surface and the atmosphere is also the most important process to include when modeling the feedback interactions between lake and climate. In addition to an obvious shortage of flux data over lake surfaces, it remains unclear whether the physical processes that govern the exchanges of water and energy during a single climatic period, or a specific location, can be extrapolated to

other time periods or other lakes. For example, a study of the surface energy budget over a larger lake (130 km<sup>2</sup>) in Mississippi, USA, showed that the diurnal change of latent heat ( $LE$ ) was correlated with the variations of wind speed and vapor pressure deficit (VPD), but not with net radiation ( $R_n$ ), whereas diurnal variations of sensible heat ( $H$ ) appeared to correlate well with the vertical temperature differences [Liu *et al.*, 2009]. These findings are not in agreement with the biophysical models developed for the terrestrial ecosystems.

Modeling studies have provided evidence that the inclusion of data from lakes can significantly improve simulations of local temperature, evaporation, and precipitation when compared to those without lake effects [Long *et al.*, 2007]. For example, the Great Lakes not only result in a phase shift in the annual cycles of latent and sensible heat fluxes but increase local evaporation and precipitation during the autumn and winter and alter air temperature gradients [Lofgren, 1997]. Despite the importance of the lakes, there lacks direct, long-term measurements on the exchange of water and energy between the lakes and the atmosphere because these exchanges are complex, costly, and extremely difficult to measure continuously [Nordbo *et al.*, 2011].

The importance of inland waters in carbon cycling has only been recently recognized [Rantakari and Kortelainen, 2005; Rouse *et al.*, 2005; Huotari *et al.*, 2011]. Historically, lakes were considered as carbon neutral or as a source to the atmosphere. This conclusion was primarily based on nonconsecutive chamber measurements [Eugster *et al.*, 2003; Heikkinen *et al.*, 2004] or ecosystem models [e.g., Cole and Caraco, 1998; Crusius and Wanninkhof, 2003; Bennington *et al.*, 2012]. Lakes may mineralize and vent to the atmosphere up to 28% of the net ecosystem CO<sub>2</sub> flux ( $F_{CO_2}$ ) of the surrounding landscape [Hanson *et al.*, 2004]. The annual CO<sub>2</sub> emissions of lakes in the boreal zone, for example, are 17–43 times higher than the effective net sedimentation of carbon [Kortelainen *et al.*, 2006]. Recent interests and field data on the roles of phytoplankton, especially in shallow lakes, caused us to reconsider the role of lakes in the regional carbon budget [Huotari *et al.*, 2011]. We challenged ourselves with a simple question: Are lakes carbon neutral or a source to the atmosphere under any conditions and at all times? Additionally, the uncertainties linked to CO<sub>2</sub> flux estimates over the lake surfaces have been accused of the paucity of accurate measurements or estimates [Jonsson *et al.*, 2008].

Studies from decades ago [Coyne and Kelley, 1974; Cole *et al.*, 1994; Liu *et al.*, 2009] and recently revisited works [Richey *et al.*, 2002; Rudorff *et al.*, 2011] indicated that lakes also serve as carbon conduits with the surrounding terrestrial systems, further emphasizing the importance of CO<sub>2</sub> exchange by lakes. However, our thorough search of the literature indicated that previous direct measurements using the eddy covariance (EC) techniques in inland water covered only short-term to year-around data [Rouse *et al.*, 2003]. Currently, few lakes and regions are equipped to consecutively measure the ecosystem-level net exchange between the Earth's surface and the atmosphere such as an EC technique [Baldocchi *et al.*, 2001; Chen *et al.*, 2004] to collect these essential data.

This study reports EC measurements taken in Western Lake Erie, a large inland body of water, and analyzes the surface latent, sensible heat fluxes, and CO<sub>2</sub> exchange that occurred during October 2011 to September 2013. We hypothesize that Lake Erie has a high  $LE$  but low  $H$  and can act as a carbon sink during algal blooms because of the high productivity of phytoplankton. We further hypothesize that coherent changes among energy, CO<sub>2</sub> fluxes, and biotic and abiotic variables do exist. Our specific study objectives are to (1) evaluate the latent and sensible heat and CO<sub>2</sub> fluxes from hourly to yearly scales and (2) explore the underlying regulations of energy and CO<sub>2</sub> fluxes from biotic and abiotic perspectives.

## 2. Materials and Methods

### 2.1. Site Description

Our study site is located in the Western Basin of Lake Erie—the fourth largest lake in North America (mean elevation 174 m above sea level), with a surface area of  $2.57 \times 10^4$  km<sup>2</sup> and a volume of 545 km<sup>3</sup>. The shallow Western Basin comprises about one fifth of Lake Erie surface area and is naturally delimited from the deeper central basin by bedrock islands, reefs, and shoals [Herdendorf and Monaco, 1988]. The Western Basin has an average depth of 5.1 m [O'Donnell *et al.*, 2010], with typically uniform water

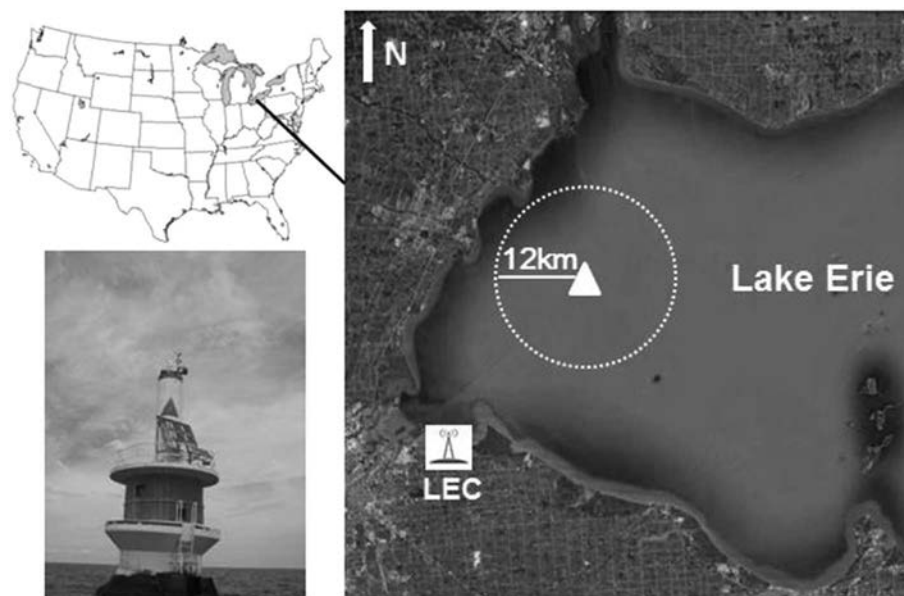


**Figure 1.** Satellite image from Google Earth (<http://www.google.com/earth/>) showing the location of the eddy covariance tower (white triangle; 41.8314°N, 83.2006°W) in Western Lake Erie. All the real time data were transmitted via the spread spectrum radio (RF450, Campbell Scientific Inc.) back to our data server at the Lake Erie Center (~25 km from the tower).

temperature and chemical composition [Guildford *et al.*, 2005]. Its waters are more sediment laden and nutrient rich than the other Lake Erie Basins and other Great Lakes due to large sediment loads from the Detroit and Maumee Rivers and from wave resuspension, which brings silt and clay from the bottom into the shallow waters [Michalak *et al.*, 2013]. Phosphorous from farmland fertilizer drains into the agriculture-dominated Maumee River system and has been implicated in the increasing prevalence of harmful algal blooms (HABs), which are dominated by the cyanobacteria (*Microcystis*) that develop during late summer months [Bridgeman *et al.*, 2013] and turn the water color in green. In August 2014, a massive algal bloom led to a ban on the City of Toledo's drinking water and affected 500,000 residents.

A permanent EC flux station, equipped with wireless capability, was installed in October 2011 at the NOAA No. 2 Light buoy (41.8314°N, 83.2006°W; Figure 1) in the Western Basin and has continually operated since then. This station is located ~12 km offshore from the north, with a water depth at ~7.5 m. The catchment area along 60 km of the Detroit River provides over 80% of the water to Lake Erie. The estuary is located 22 km northeast of our site. This catchment and the lakeshore surroundings include urban buildings, croplands, and forests.

## 2.2. Eddy Covariance and Meteorological Measurements

An open-path EC system was installed to measure  $LE$ ,  $H$ , and  $F_{CO_2}$  between the lake surface and the atmosphere at ~15 m above lake water elevation. It contains an infrared gas analyzer (IRGA, Model LI-7500A, LI-COR, Lincoln, NE, USA) and a CSAT3 three-dimensional sonic anemometer (Campbell Scientific Inc. CSI, Logan, UT, USA). The three-dimensional wind velocities, sonic temperature, and  $CO_2$  and  $H_2O$  concentrations were sampled at a 10 Hz frequency, and the raw time series (TS) data were stored in a CR3000 data logger (CSI). The IRGA was calibrated before the start of the campaign in 2011 and rotated routinely during maintenance trips in 2012 and 2013. Micrometeorological variables included photosynthetically active radiation (PAR) (LI-190, LI-COR), relative humidity (RH), and air temperature ( $T_a$ ) (HMP45C, CSI), which were measured at the same height as the EC system. Rainfall was measured with a tipping bucket rain gauge (TE-525, CSI). The half hourly micrometeorological data were recorded by the CR3000 data logger. The 10 Hz TS data and half hourly data were transmitted via the spread spectrum radio (RF450, equipped with a 14201 Yagi directional antenna, CSI) back to our data server at the Lake Erie Center (~25 km from the tower; Figure 1). We set the radio system to transmit the data every 5 min so that the instrumental conditions are monitored on a near real-time basis.

### 2.3. Biophysical Measurements

Water quality properties and microclimatic variables within the footprint of the EC tower were measured. A YSI 6600 water quality sonde was used to collect water column data at approximately biweekly intervals depending on the weather from early April to late September in both years. The 0–1.0 m water column was sampled for temperature, pH, and chlorophyll *a*. At the same time, two 50 mL replicate water samples were filtered on glass-fiber filters. The filters were desiccated and stored in an ultracold freezer ( $-70^{\circ}\text{C}$ ). Chlorophyll *a* was then extracted from the filters using dimethylformamide and analyzed fluorometrically on a Turner fluorometer [Inskip and Bloom, 1985]. These results were used to cross validate YSI 6600 measurements on chlorophyll *a*. In order to measure HABs of the cyanobacterium (*Microcystis*), plankton tows were collected at each site between 9:00 h and 16:00 h in vertical tows from near the lake bottom to the surface using a 0.5 m diameter, 112  $\mu\text{m}$  mesh net that is equipped with a flowmeter to calculate net efficiency. All plankton tows were concentrated to a volume of 100–500 mL and immediately preserved in 4% buffered (pH = 7.5) sugar formalin. All tows were collected in duplicates and stored in the laboratory at room temperature until analysis for biovolume of *Microcystis* [Bridgeman *et al.*, 2013]. Data from Aqua Moderate Resolution Imaging Spectroradiometer (MODIS)'s remote sensing of the chlorophyll *a* were also used in this analysis for a long-time series variation. We included land/cloud bands to compute a 250 m resolution of chlorophyll *a* (Level 2) by the SeaDAS from MODIS Level 1 data. We kept the OC3 for standard 1 km resolution products by NASA as our retrieval algorithm [O'Reilly, 2000].

### 2.4. Flux Calculation, Quality Assurance/Quality Control, and Gap Filling

Half hourly  $LE$ ,  $H$ , and  $F_{\text{CO}_2}$  were calculated by using the EdiRe (University of Edinburgh, v1.5.0.32, <http://www.geos.ed.ac.uk/abs/research/micromet/EdiRe>) following the workflow described in Chu *et al.* [2013, 2014a, 2014b]. Briefly, raw TS data quality was checked, and spikes were removed [LI-COR, 2004]. The diagnostic signals from the CSAT3 and LI-7500A were used to flag periods with instrument malfunction. Time lags between measured scalars and vertical velocity were removed, and the planar fit method was applied to rotate the three velocity components into the mean streamline coordinate system [Wilczak *et al.*, 2001]. The raw sonic temperature was corrected with fluctuations of water vapor concentration. A 30 min blocking average without detrending was used [Moncrieff *et al.*, 2004], and a Webb-Pearman-Leuning correction was applied to correct air density fluctuation of the air. The stationarity, integral turbulence characteristics, and friction velocity ( $u^*$ ) of each 30 min flux were calculated to filter out the periods with poor turbulent development [Foken and Wichura, 1996]. The  $u^*$  threshold was set at  $0.1 \text{ m s}^{-1}$ . We set experiential range checks for each of the physical variables. We also adopted a 7 day moving window in the time series of half hourly fluxes in order to detect and filter out the erroneous flux ( $>6$  times standard deviation of each window). Finally, the footprint for each half hourly flux was calculated and used to omit periods with  $<80\%$  of the measured fluxes originated within measurement fetch (see footprint analysis).

Cospectra of temperature,  $\text{H}_2\text{O}$ , and  $\text{CO}_2$  with the vertical wind speed were calculated in order to examine the turbulence characteristics and assess the data quality. Cospectral analysis is widely used to identify artificial noise that could result in erroneous data and to determine the sensors reasonably resolve high frequencies [Ikawa *et al.*, 2013]. When the sensors accurately resolve high-frequency contributions to the covariance, the logarithmic cospectra of  $\text{H}_2\text{O}$  and  $\text{CO}_2$  with the vertical wind speed according with the cospectra of temperature with the vertical wind speed follow a  $-1.333$  slope against normalized frequency of the site (Figure 2). We found that the temperature,  $\text{H}_2\text{O}$ , and  $\text{CO}_2$  cospectra had the expected shape, with only a slight high-frequency attenuation. Thus, correction procedures for high-frequency losses were not needed.

There were 36%, 50%, and 35% of  $LE$ ,  $H$ , and  $F_{\text{CO}_2}$ , respectively, that passed the quality checks as described above. The similar data gaps were also shown in Ikawa *et al.* [2013] and Podgrajsek *et al.* [2014b] in aquatic flux measurements. About 14% of our data gaps resulted from the occasional malfunction of sonic anemometer during heavy rainfall and snowfall periods. Power supply shortage and failure in data transmission accounted for 4% of the data gaps. Nonideal meteorological conditions (e.g., stable, nonstationary, and weak turbulent development) eliminated an additional 31%, 26%, and 34%, and the footprint criterion and physical variable range eliminated the other 15%, 6%, and 13% for  $LE$ ,  $H$ , and  $F_{\text{CO}_2}$ , respectively.

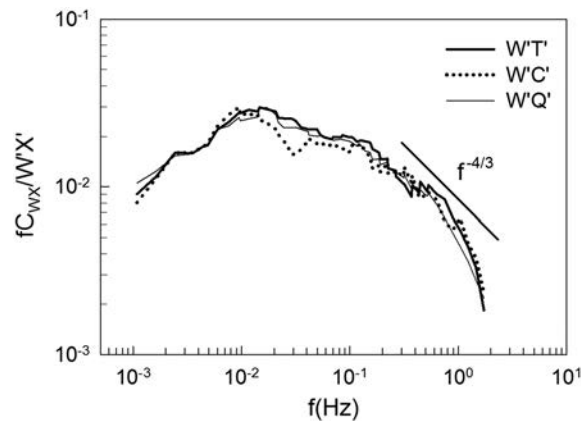


**Figure 2.** Normalized cospectra ( $W'X$ ) of the vertical wind speed, with temperature ( $W'T$ ),  $\text{CO}_2$  density ( $W'C$ ), and  $\text{H}_2\text{O}$  density ( $W'Q$ ) for the eddy covariance data obtained from Western Lake Erie. Data were derived from DOY 200–212 in the summer, with only data collected during unstable conditions (i.e., Monin-Obukhov stability parameter  $z/L < -0.01$ ). The theoretical  $-1.333$  slope of the inertial subrange is denoted by the separate thick line.

following two reasons: (1) water and  $\text{CO}_2$  fluxes at lake ecosystems were noted as less directly coupled with the phytoplankton succession than terrestrial ecosystems dynamics [Vesala *et al.*, 2006] and (2) the MDS approach took advantages of the autocorrelation structure in flux data and incorporated the self-dependency in filling the gaps [Reichstein *et al.*, 2005], providing a robust approach for integrating the daily, monthly, or annual fluxes. Briefly, the gaps of fluxes were filled by the following steps: (1) the linear interpolation was applied to gaps less than 1.5 h, (2) the remaining gaps were filled with the mean half hourly values with similar micrometeorological conditions (PAR, VPD, and  $T_a$ ) within a given window size around the gaps, and (3) the gaps were filled with the mean diurnal values from a given window size around the gaps when micrometeorological data were unavailable. The window size increased from 7, 14, 28, to 56 days through the iterations of (2) and (3). The gap-filled data were used while integrating the half hourly  $LE$ ,  $H$ , and  $F_{\text{CO}_2}$  into daily, monthly, seasonal, and annual values. Positive values of  $F_{\text{CO}_2}$  indicated a  $\text{CO}_2$  source to the atmosphere, and the negative values indicated a  $\text{CO}_2$  sink by the lake.

### 2.5. Footprint and Uncertainty Analysis

The source area of each half hourly flux was calculated by using the footprint model from Kormann and Meixner [2001]. Specifically, we targeted the cumulative flux contribution from the areas that are 0–1, 1–2, 2–4, and 4–12 km from the tower location. The model simulation showed that 63%, 75%, and 80% of the cumulative fluxes were contributed by areas within a 1, 2, and 4 km radius, respectively, centering our tower throughout the study period. Since our tower is located 12 km away from the nearest shore, the influences of terrestrial ecosystems on our flux measurements appeared negligible. Thus, our measured fluxes can adequately represent the  $\text{CO}_2$  and energy exchanges of the lake.

Uncertainties of fluxes generated from the flux calculation, gap-filling processes, and  $u^*$  criterion selection were estimated following Aurela *et al.* [2002]. Briefly, the random error for each half hourly flux was estimated following Chu *et al.* [2014a]. The errors were propagated through the gap-filling processes and incorporated into the uncertainties of the gap-filling data [Reichstein *et al.*, 2005]. The Monte Carlo simulations ( $N=1000$ ) technique was adopted following Chu *et al.* [2014b]. The uncertainties of the  $u^*$  criterion selection were estimated by the sensitivity analysis of applying different  $u^*$  criterion. Finally, the half hourly uncertainties were integrated into annual sums. In addition, three gap-filling methods were compared for verifying the MDS method and for quantifying the gap-filling uncertainties. Unless specified, all the flux uncertainties were reported as confidence intervals (CI, 95%).

The monthly mean actual measurement quality assurance control (QAC) and the other two major gap-filling methodologies [Falge *et al.*, 2001b] of mean diurnal variation (MDV) and marginal distribution sampling (MDS) were used to fill the data gaps in  $LE$ ,  $H$ , and  $F_{\text{CO}_2}$ , in order to calculate the daily to annual integrals of these fluxes because there is no single, accepted method for processing flux data in aquatic systems. QAC combines all the quality assurance and quality-controlled data using monthly mean and is similar to the chamber inconsecutive measurement but with higher frequency. Unlike the MDS method, the MDV method takes no account of day-to-day variations in weather conditions [Falge *et al.*, 2001a]. The MDS method was adopted for the

## 2.6. Estimation of Net Radiation ( $R_n$ )

The  $R_n$  sensor was mounted in September 2013, a later date than the other flux sensors. When the  $R_n$  was not available, it was estimated to analyze the role of  $LE$  in energy partitioning and as a threshold to check the quality of  $LE$  data based on the procedure outlined in *Allen et al.* [1998]:

$$R_n = R_{ns} - R_{nl} \quad (1)$$

where  $R_{ns}$  is the net incoming shortwave radiation and  $R_{nl}$  is the net outgoing longwave radiation. Their units are in  $\text{MJ m}^{-2} \text{d}^{-1}$ .

$R_{ns}$  is estimated from the measured incoming solar radiation ( $R_g$ ,  $\text{MJ m}^{-2} \text{d}^{-1}$ ) at another flux tower nearby also in Western Lake Erie Basin at  $\sim 10$  km north:

$$R_{ns} = (1 - \alpha)R_g \quad (2)$$

where  $\alpha$  is the shortwave albedo of the water surface set to 0.08 based on direct measurements made around the tower.

$R_{nl}$  is estimated by

$$R_{nl} = \sigma \left( 0.34 - 0.14 \sqrt{\bar{v}_a} \right) \left( \frac{(T_{\max} + 273.2)^4 + (T_{\min} + 273.2)^4}{2} \right) \left( 1.35 \frac{R_g}{R_{so}} - 0.35 \right) \quad (3)$$

where  $R_{so}$  is the clear-sky radiation ( $\text{MJ m}^{-2} \text{d}^{-1}$ ).  $\bar{v}_a$  is the mean actual daily vapor pressure (kPa),  $T_{\max}$  and  $T_{\min}$  are, respectively, the maximum and minimum daily air temperature ( $^{\circ}\text{C}$ ), and  $\sigma$  is Stefan-Boltzmann constant ( $\text{MJ K}^{-4} \text{m}^{-2} \text{d}^{-1}$ ).

$$R_{so} = (0.75 + 2 \times 10^{-5} \text{Elev}) R_a \quad (4)$$

where  $Elev$  is the ground elevation (m) above mean sea level of the flux station and  $R_a$  is the extraterrestrial radiation ( $\text{MJ m}^{-2} \text{d}^{-1}$ ), which is the solar radiation on a horizontal surface at the top of the Earth's atmosphere and is computed by

$$R_a = \frac{1440}{\pi} \times 0.0820 \times d_r^2 [\omega_s \sin(lat) \sin(\delta) + \cos(lat) \cos(\delta) \sin(\omega_s)] \quad (5)$$

where  $0.0820 \text{ MJ m}^{-2} \text{min}^{-1}$  is the solar constant and  $d_r$  is the inverse relative distance.

Earth-Sun  $\omega_s$  is the sunset hour angle (rad),  $lat$  is the latitude (rad), and  $\delta$  is the solar declination (rad).

$$d_r^2 = 1 + 0.033 \times \cos \left( \frac{2\pi}{365} \text{DOY} \right) \quad (6)$$

Equations (5) and (6) were modified from the errata of *Chen et al.* [1993] and *Allen et al.* [1998]. DOY is day of year.

$$\delta = 0.409 \times \sin \left( \frac{2\pi}{365} \text{DOY} - 1.39 \right) \quad (7)$$

The sunset hour angle  $\omega_s$  is estimated from

$$\omega_s = \arcsin[-\tan(lat)\tan(\delta)] \quad (8)$$

## 2.7. Data Analysis

To present the seasonal changes of  $\text{CO}_2$  and energy fluxes and to provide annual sums, we divided the data set into 2 years: December 2011 to September 2012 (Year 1) and December 2012 to September 2013 (Year 2). To determine the diurnal changes of energy (Figure 5) and  $\text{CO}_2$  (Figure 6) fluxes, all of the quality-controlled data were combined into 30 min averages on a monthly scale. This was done to reduce the sampling error associated with individual flux measurements that result from the intermittent, natural state of turbulence caused by horizontal transport across large sunny and shaded patches [*Baldocchi et al.*, 2000; *Blanken et al.*, 2011].

The planar fit coordinate procedure, gap-filling procedures, and other statistical analyses were accomplished with R language (R Development Core Team, 2013 version 3.0.0). Remote sensing data processes were conducted in SeaDAS 7.1 and ENVI 5.1.

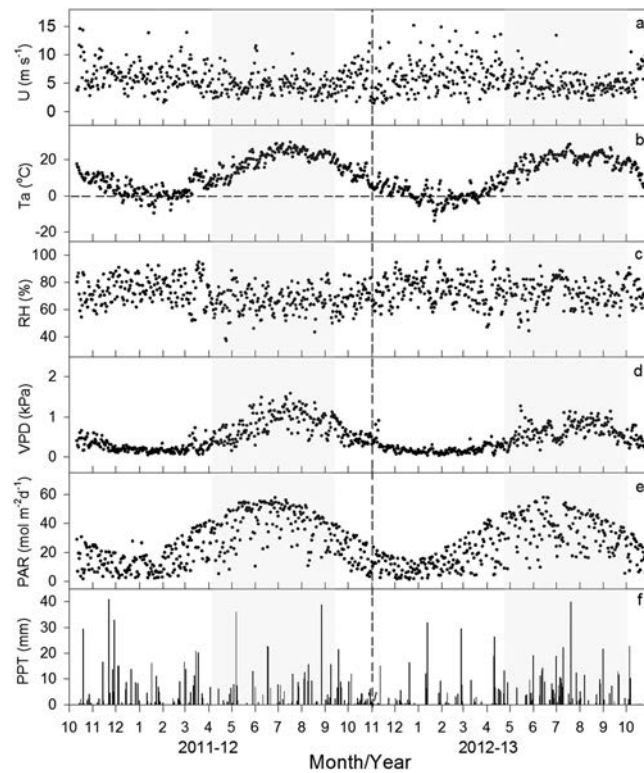


**Figure 3.** (a) Mean daily wind speed ( $U$ ), (b) air temperature ( $T_a$ ), (c) relative humidity (RH), (d) vapor pressure deficit (VPD), (e) photosynthetically active radiation (PAR), and (f) daily rainfall at ~15 m above the water surface in Western Lake Erie from October 2011 to September 2013.

varied from 40 to 60 mm during May–October (Figure 3f). Total annual rainfall was 810 and 740 mm in Year 1 and Year 2, respectively, excluding snowfall during freezing conditions when the rain gauge failed to work. The lake also has characteristically strong winds, moving from northwest to east/west throughout the year. Usually, lake effect snow starts from November as the cold winds of winter pass over the warm waters, with the snow melting after February. The NOAA’s real-time camera (<http://www.glerl.noaa.gov/metadata/tol2/>) recorded no frozen coverage at our site in Year 1, with ice cover from 16 February to 7 March in Year 2 (Table 1). Year 2 was significantly ( $P < 0.05$ ) colder and more cloud cover than in Year 1.

### 3. Results

#### 3.1. Climatic, Meteorological, and Water Property Conditions

The air temperature ( $T_a$ ), vapor pressure deficit (VPD), and photosynthetically active radiation (PAR) showed a unimodal change at annual scale (Figures 3b, 3d, and 3e). Peak  $T_a$ , VPD, and PAR values were recorded in June, July, and August, while lower values were recorded in January and December in both years. The annual mean  $T_a$ , VPD, and PAR values were 12.19 and 10.44°C, 0.53 and 0.41 kPa, and 27.5 and 25.1 mol m<sup>-2</sup> d<sup>-1</sup> for Year 1 and Year 2, respectively. Wind speed ( $U$ ) averaged 5.6 m s<sup>-1</sup> (Figure 3a and Table 1), with synoptic weather events driving  $U$  to a maximum of 15.0 m s<sup>-1</sup> (Figure 3a). Rainfall precipitation showed little monthly variability, ranging from 50 to 70 mm from May to October in Year 1, with a greater precipitation near 100 mm in August. In Year 2, precipitation reached a high of 100 mm in June and 150 mm in July, with higher RH, lower VPD, and PAR in these 2 months (Figures 3c, 3d, and 3e). Precipitation

**Table 1.** Daily Means of Major Meteorological Variables for Western Lake Erie From October 2011 to September 2013<sup>a</sup>

Items	May–September		October–April		Entire Year	
	2012	2013	2011–2012	2012–2013	2011–2012	2012–2013
$U$ (m s <sup>-1</sup> )	4.77	4.84	6.11	6.20	5.56	5.63
$T_a$ (°C)	21.3	20.0	5.3	3.6	12.2	10.4
RH (%)	67.0	71.9	72.8	74.1	70.4	73.2
VPD (kPa)	0.87	0.67	0.29	0.23	0.53	0.41
PAR (mol m <sup>-2</sup> d <sup>-1</sup> )	40.6	36.8	18.0	16.7	27.5	25.1
Rainfall (mm, summed)	360	400	450	340	810	740
$E$ (mm)	3.19	2.62	1.09	1.16	1.97	1.77
$\beta$	0.26	0.16	0.79	0.52	0.40	0.26
Frozen up					No frozen	16 Feb
Ice out					No frozen	7 Mar
Water depth (m)					7.5	7.5

<sup>a</sup> $U$ , mean daily wind speed;  $T_a$ , air temperature; RH, relative humidity; VPD, vapor pressure deficit; PAR, photosynthetically active radiation; rainfall, summed rainfall;  $E$ , evaporation;  $\beta$ , mean midday Bowen ratio. Midday was defined as 10:00 h–15:00 h local eastern standard time.

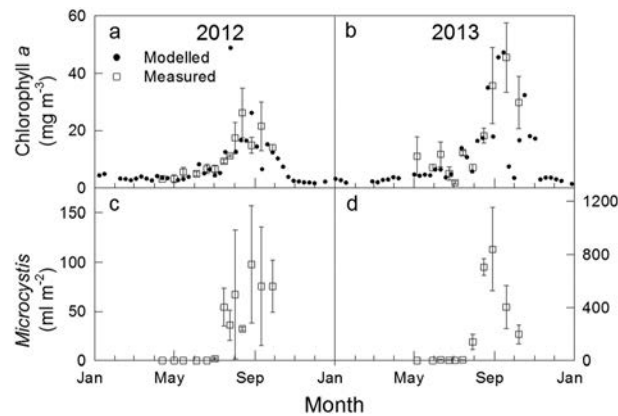


**Figure 4.** Seasonal variation (mean  $\pm$  standard deviation) of (a and b) chlorophyll *a* content and (c and d) *Microcystis* biovolume for Western Lake Erie in 2012 and 2013. Remote sensed weekly mean chlorophyll *a* content (MODIS OC3 algorithm, see method) was also shown.

Both chlorophyll *a* content and *Microcystis* biovolume showed one-peak seasonal change (Figure 4). The chlorophyll *a* content of surface water increased gradually from April and peaked in September with a fast growth of algal bloom in late summer and fall in both years. There was a decrease in the measured chlorophyll *a* content and *Microcystis* biovolume in August of Year 1. The highest chlorophyll *a* content was recorded in September 2013 at  $45.6 \pm 12.1$  (standard deviation)  $\text{mg m}^{-3}$ , which was 1.8 times greater than the lower chlorophyll *a* in 2012. The annual mean chlorophyll *a* content of the surface water was  $11.1 \pm 2.0$ ,  $16.9 \pm 4.3 \text{ mg m}^{-3}$  and pH was  $8.4 \pm 0.3$ ,  $8.5 \pm 0.3$  in 2012 and 2013, respectively.

*Microcystis* appeared in early July, with an annual mean biovolume of  $34 \pm 10$  and  $210 \pm 93 \text{ mL m}^{-2}$  in Year 1 and Year 2, respectively, amounting to 6.2 times greater in 2013 than that in 2012.

### 3.2. Diurnal Changes in *LE*, *H*, and $F_{\text{CO}_2}$

*LE* had noticeable diurnal changes in July–September (Figure 5). The maximal *LE* ( $130\text{--}150 \text{ W m}^{-2}$ ) was recorded in July–September, whereas the minimal *LE* ( $0\text{--}30 \text{ W m}^{-2}$ ) was found in December–March in both years. Hourly *LE* varied from  $-10$  to  $180 \text{ W m}^{-2}$ . Interestingly, we found higher *LE* at night than that during the day in June–September (Figures 5i–5l), especially in July and September (Figures 5j and 5l). In Year 1, the lowest *LE* in July–September occurred at noon, except the rainy and cloudy August (Figures 5j and 5l). During the two summer months, the diurnal *LE* fluctuation was higher than that in other months, with  $50 \text{ W m}^{-2}$  in the daytime and  $180 \text{ W m}^{-2}$  at night (i.e.,  $130 \text{ W m}^{-2}$  difference).

*H* also had noticeable diurnal changes in spring and autumn (Figure 5). The daily differences of *H* were much lower than those of *LE*. The maximal *H* ( $20\text{--}40 \text{ W m}^{-2}$ ) was recorded in spring and autumn (Figures 5g, 5l, 5a, and 5h), whereas the minimal *H* ( $-17\text{--}0 \text{ W m}^{-2}$ ) was recorded from October to March in both years (Figures 5a–5f). Specifically, the hourly *H* varied from  $-17 \text{ W m}^{-2}$  (November 2011) to  $40 \text{ W m}^{-2}$  (September 2012). *H* was at a minimum in the afternoon (15:00–17:00 h) and peaked in the early morning (7:00–9:00 h) in July–September (Figures 5j–5l). The diurnal amplitude of *H* was the largest in the spring and early fall ( $30 \text{ W m}^{-2}$  in September), low in July and August ( $20 \text{ W m}^{-2}$ ).

Similar to *LE*,  $F_{\text{CO}_2}$  had clear diurnal changes in August and September during the high chlorophyll *a* period (Figure 6 versus Figure 4). A maximal  $F_{\text{CO}_2}$  release ( $12.19 \mu\text{mol m}^{-2} \text{ s}^{-1}$ ) and uptake ( $-7.34 \mu\text{mol m}^{-2} \text{ s}^{-1}$ ) were observed during this period (Figures 6d, 6e, 6j, and 6k). The diurnal  $F_{\text{CO}_2}$  variation appeared lower in other months or without any noticeable differences over time. The carbon uptake hours occurred in the early morning in some months (Figures 6a, 6c, 6e, 6i, 6k, and 6l).

### 3.3. Seasonal Changes in *LE*, *H*, and $F_{\text{CO}_2}$

There were clear, unique seasonal changes in *LE*, *H*, and  $F_{\text{CO}_2}$  (Figure 7). *LE* showed an obvious one-peak change in both years. *LE* was lower (near zero) from November to February during both winters. In both years, at the beginning of March, *LE* switched to a positive value and continued to increase, reaching a maximum in July–September. The maximal *LE* appeared in late July, with  $22.73$  and  $20.81 \text{ MJ m}^{-2} \text{ d}^{-1}$  in Years 1 and 2, respectively. *LE* decreased after mid-September and reached an extremely low level after November. Another noticeable decrease (Figure 7a) was recorded in June and July in Year 2, which coincided with the continuous rain events (Figure 3f). Based on the MDS method, the annual cumulative *LE* was  $\sim 1765 \pm 46$  ( $\pm 95\%$  CI) and  $1580 \pm 76 \text{ MJ m}^{-2}$  (i.e.,  $720 \pm 19$  and  $645 \pm 31 \text{ mm}$ ), compared with an annual rainfall of 810 and 740 mm in Year 1 and Year 2, respectively.

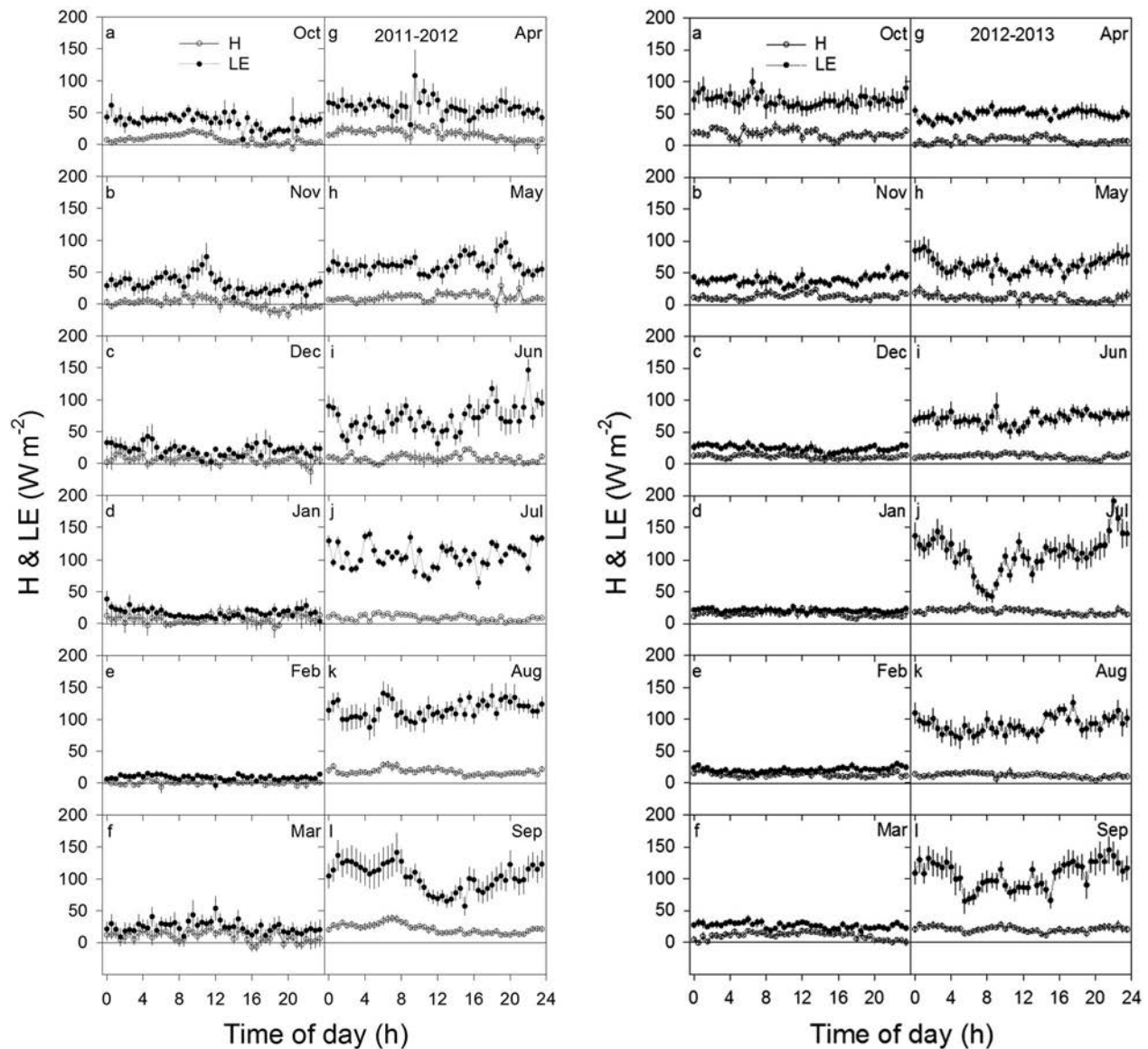


**Figure 5.** Monthly average diurnal course of sensible (*H*) and latent (*LE*) heat fluxes for Western Lake Erie from October 2011 to September 2012 and from October 2012 to September 2013 (with continued figure).

This suggests that ~90% of annual rainfall returned to the atmosphere through evaporation at our site. The *LE* in Year 2 was lower than that in Year 1, which was consistent with the climatic differences that showed Year 2 to be significantly ( $P < 0.05$ ) colder and more cloudier than Year 1.

Periodic changes appeared at monthly scales and increased from summer to late autumn in *H* (Figure 7b). The daily *H* ranged from  $-2.95$  to  $8.37 \text{ MJ m}^{-2} \text{ d}^{-1}$ , with relatively small values in the warm season and large values in the cool season. Annual *H* was  $340 \pm 19$  and  $380 \pm 19 \text{ MJ m}^{-2}$  in Year 1 and 2, respectively, which is ~25% of the annual *LE*.

Western Lake Erie acted as a small carbon sink in the summer and as a carbon source in the winter (Table 2), with greater  $F_{\text{CO}_2}$  variations in both summers (Figure 7d). It varied from  $-0.45 \text{ g C m}^{-2} \text{ d}^{-1}$  (July) to  $0.61 \text{ g C m}^{-2} \text{ d}^{-1}$  (March) in Year 1 and from  $-0.36$  (September) to  $0.98 \text{ g C m}^{-2} \text{ d}^{-1}$  (April) in Year 2. Its fluctuation, however, did not appear correlated with the changes in  $T_a$  or PAR (Figures 3b and 3e and Figure 7), which are the relationships often found in terrestrial ecosystems. At annual scale, the Lake Erie acted as a carbon source of  $77.7 \pm 18.6$  and  $49.5 \pm 17.9 \text{ g C m}^{-2} \text{ yr}^{-1}$  in the first and second years,

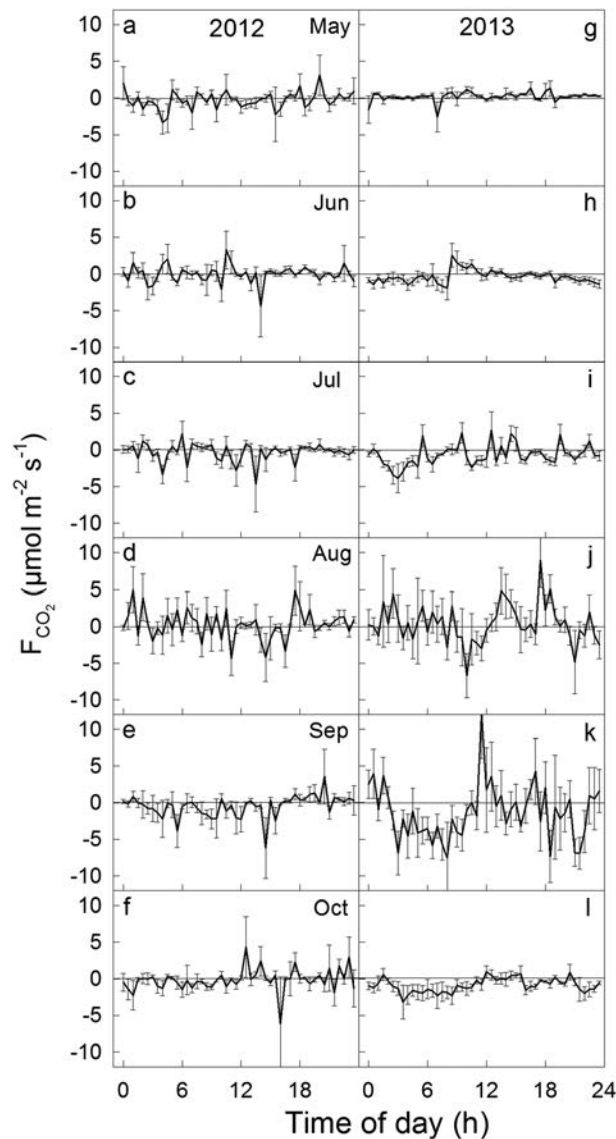


**Figure 6.** Monthly average diurnal course of CO<sub>2</sub> fluxes ( $F_{CO_2}$ ) for Western Lake Erie from May to October in 2012 and 2013. The bars represent twice the standard error for each half hourly mean in a month (95% confidence interval).

*et al.*, 2013; Podgrajsek *et al.*, 2014b] were larger (~10–20%) than those in terrestrial ecosystems after data quality control, the data gaps were not large and appeared spreading out through the study period. After filling gaps that were less than 1.5 h, there were 40% gaps in  $H$  and 49% in  $LE$  and  $F_{CO_2}$ , respectively. However, after filling the short-term (1–2 weeks) fluxes with similar meteorological conditions, there were only 5% gaps in  $H$  and 6% in  $LE$  and  $F_{CO_2}$ , respectively.

In the MDS method, PAR, VPD, and  $T_a$  were selected as the class indicators [Falge *et al.*, 2001a; Falge *et al.*, 2001b] to fill the gaps in  $LE$ ,  $H$ , and  $F_{CO_2}$ . These variables are the most fundamental ones for the aerodynamic method and are widely applied in numerical lake models, especially for  $LE$  and  $H$  [Nordbo *et al.*, 2011]. We examined the relationships between  $H$ ,  $LE$ , and a variety of environmental factors and identified a suite of significant factors (Figure 9). We also considered  $U$  as an important driving force. However, the turbulent fluxes did not correlate well with wind speed alone. Although there were significant ( $P < 0.0001$ ) relationships between  $LE$  and the product of  $U$  and VPD and between  $H$  and the product of  $U$  and  $\Delta T$ , the single VPD or  $\Delta T$  performed better than or similar to their product with  $U$  [see also

respectively, but as a weak carbon sink of  $-19.0 \pm 5.4$  and  $-40.2 \pm 13.3 \text{ g C m}^{-2}$  in the first and second summers (May–September).

## 4. Discussion

### 4.1. Gap-Filling Method Selection and Uncertainties

The results and their uncertainties reported in this paper rely greatly on the gap-filling methods because of the existing large data gaps. We found satisfactory and consistent monthly and yearly between the two gap-filling methodologies (i.e., MDS and MDV) [Falge *et al.*, 2001b] and monthly mean actual measurement (QAC; Figure 8 and Figure S1 in the supporting information). The uncertainties among the three methods were 4%, 6%, and 10% for  $LE$ ,  $H$ , and  $F_{CO_2}$ , respectively, with higher uncertainties in  $F_{CO_2}$  than those in energy fluxes. Our annual  $LE$  uncertainty is within 0.6%–5% when using different gap-filling methods as reported by others [Falge *et al.*, 2001a; Alavi *et al.*, 2006], indicating a small effect on our seasonal/annual results. The annual sums that result from the QAC method were greater than by those from both the MDS and MDV methods for energy fluxes (Figures 8a, 8b, 8d, and 8e). Similar to Falge *et al.* [2001a], we also found that the annual sums resulting from filling by the MDS method were in general slightly smaller than data filled by the MDV method (Figures 8b, 8d, and 8e). Although the measurement data gaps in our aquatic study and others [Ikawa

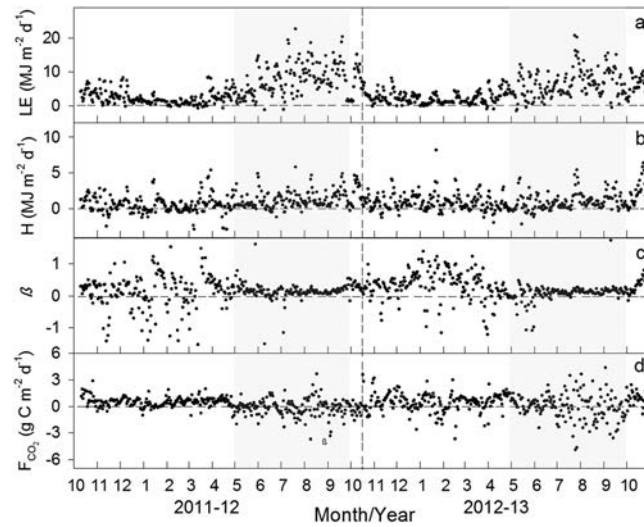


**Figure 7.** (a) Seasonal changes of daily latent ( $LE$ ), (b) sensible ( $H$ ) heat fluxes, (c) Bowen ratio ( $\beta$ ), and (d)  $CO_2$  flux ( $F_{CO_2}$ ) for Western Lake Erie from 2011 to 2013 by using the marginal distribution sampling (MDS) gap-filling method.

from those in small lakes or in terrestrial ecosystems [e.g., Shao et al., 2008]. Similar magnitudes of the diurnal changes in  $LE$  were found at a large open reservoir in Mississippi [Liu et al., 2009] and in an Amazon floodplain lake [Polsenaere et al., 2013]. Similar magnitudes of hourly  $LE$  ( $\sim 0\text{--}200\text{ W m}^{-2}$ ) and  $H$  ( $\sim -50\text{--}50\text{ W m}^{-2}$ ) were also found over a northern Great Slave Lake in Canada [Blanken et al., 2000]. Considering as a potential evapotranspiration capacity of the region, the maximum  $LE$  at our lake site was  $21.77\text{ MJ m}^{-2}\text{ d}^{-1}$ , which was much higher than that for a forest without water limitations with a maximum  $LE$  of  $13.48\text{ MJ m}^{-2}\text{ d}^{-1}$  in the adjacent watershed [Xie et al., 2014], i.e., 1.6 times greater  $LE$  in the lake than that in the forest.

As a result, the seasonal change in the Bowen ratio ( $\beta$ ,  $H/LE$ ) had greater winter and lower summer values (Figure 7) due to low  $LE$  in the winter, and high  $LE$  in the summer, with stable  $H$  throughout the year. The  $LE$  clearly exceeded the  $H$  during spring and summer (i.e.,  $\beta < 1$ ; Figure 7), suggesting that the energy absorbed by the water was consumed through evaporation. Our results showed that April and October shared higher  $\beta$  of  $\sim 0.5$  (i.e., relative higher  $H$  accompanied with the lower  $LE$ ) than other growing season months. We also found a summer average  $\beta$  of 0.14 when the  $R_n$  consumed by  $LE$  was 7 times more than by  $H$  during the summer of the high  $R_n$  period in a year. This stable ratio and low variation in daily and seasonal  $H$  have important implications on ecosystem modeling (e.g., modeling lake water level [Gronewold et al., 2013]) when data are available at discrete time points.

Negative  $LE$  and  $H$  were only observed in several days during the spring months (Figures 5a–5g). Negative  $LE$  and  $H$  occasionally occurred when the air temperature was higher than the water surface temperature, and when the vapor pressure of the air was higher than the water surface, which indicates the influence of warmth and moisture in air masses. Under these circumstances, the atmospheric surface layer over the water was stably stratified, and turbulent exchanges of fluxes were suppressed. As such, all  $R_n$ ,  $H$ , and  $LE$

Blanken et al., 2011; Nordbo et al., 2011]. This means that the same gap-filling procedure from Falge et al. [2001a, 2001b] for terrestrial ecosystems can be adequately applied for aquatic systems. But due to the complex biotic and abiotic influences, especially on  $F_{CO_2}$ , significant efforts in exploring new gap-filling methods are needed in future research.

#### 4.2. Latent Heat and Sensible Heat Fluxes

$LE$  had high values and clear diurnal changes during the summer periods (Figure 5), whereas  $H$  showed less variation at both daily and seasonal scales. These variations in  $LE$  and  $H$  were comparable to other reported results over large lakes [e.g., Liu et al., 2009] but were remarkably different

**Table 2.** Seasonal Changes of Daily Means of Latent Heat ( $LE$ ), Sensible Heat ( $H$ ), and  $CO_2$  Fluxes ( $F_{CO_2}$ ), With Standard Error in Parentheses, at the Sampling Site in Western Lake Erie

Period	$LE$ ( $\text{MJ m}^{-2}\text{ d}^{-1}$ )	$H$ ( $\text{MJ m}^{-2}\text{ d}^{-1}$ )	$F_{CO_2}$ ( $\text{g C m}^{-2}\text{ d}^{-1}$ )
2012(May–Sept)	7.82(2.39)	1.28(0.31)	−0.12(0.32)
2013(May–Sept)	6.43(1.65)	1.45(0.47)	−0.26(0.32)
2011–2012(Oct–Apr)	2.68(1.50)	0.69(0.52)	0.27(0.13)
2012–2013(Oct–Apr)	2.83(1.60)	0.78(0.23)	0.42(0.22)
2011–2012	4.82(3.21)	0.93(0.53)	0.21(0.40)
2012–2013	4.33(2.41)	1.05(0.47)	0.14(0.33)

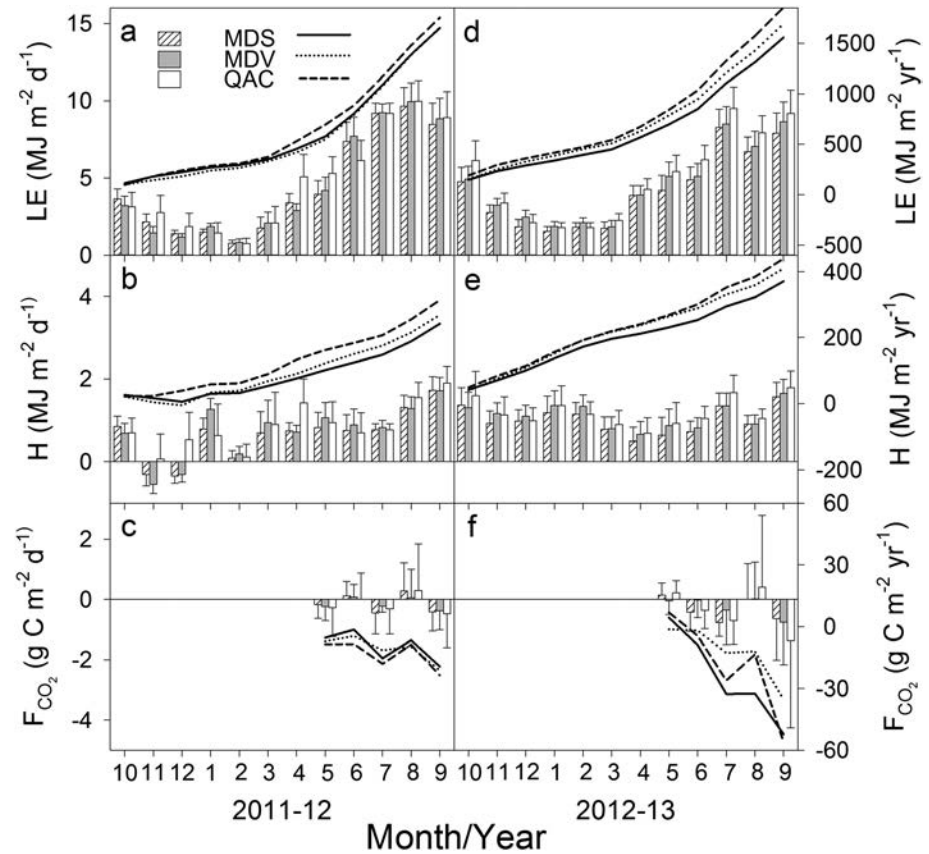


**Figure 8.** Monthly mean (bar charts with the left y axis) and seasonal/yearly accumulative (line charts with the right y axis) (a and d) latent ( $LE$ ), (b and e) sensible ( $H$ ) heat fluxes, and (c and f)  $CO_2$  fluxes ( $F_{CO_2}$ ) for Western Lake Erie from October 2011 to September 2013. Three gap-filling methodologies including marginal distribution sampling (MDS), mean diurnal variation (MDV), and monthly mean actual measurement (QAC) were used in filling the data gaps. The error bars show  $\pm 1$  SE.

were used to heat the water, with the turbulent energy  $H$  and  $LE$  decreased to negative, and thus, the water surface temperature slightly increased during this period [Liu *et al.*, 2009].

The present lake  $LE$  returned approximately 90% of the annual rainfall to the atmosphere, with an annual mean evaporation of 685 mm compared to a 775 mm rainfall. Blanken *et al.* [2000] measured a cumulative evaporation of 485 mm over the ice-free season (June–December) from a high-latitude Great Slave Lake in Canada, which is slightly lower than our measurement of 515 mm during the same season, likely due to difference in latitude and climate. As an important local atmospheric moisture source, the portion of returned  $LE$  would affect vegetation distribution and productivity, climate, and water resources across multiple spatial-temporal scales [Xiao *et al.*, 2013]. This 1.88 mm/d evaporation means that Lake Erie’s entire water loss through evaporation was  $5 \times 10^{10}$  kg  $H_2O$   $d^{-1}$ , which is equivalent to 2 times the runoff from Niagara Falls per day. It is known that evaporation rather than precipitation is the primary driver of lake level decrease, as warmer air and water temperatures and a shorter duration of ice cover favor increased rates of evaporation [Lofgren *et al.*, 2002]. The water levels of Lake Erie dropped significantly in 1997–2000, despite relatively stable annual precipitation and an inlet from other lakes, indicating that the lake evaporation plays a dominant role in the water level of the Great Lakes [Gronewold *et al.*, 2013].

**4.3. Linking Energy and  $CO_2$  Fluxes With Driving Forces**

The turbulent exchange of  $LE$  and  $H$  are governed by several meteorological factors including the magnitude of VPD, difference in temperature between the water and the atmosphere, and the turbulent mixing [Nordbo *et al.*, 2011] through direct physical regulation processes. Significant correlations were found between meteorological factors and  $LE$  or  $H$  (Figure 9 and Figure S2 in the supporting information). Half hourly  $LE$

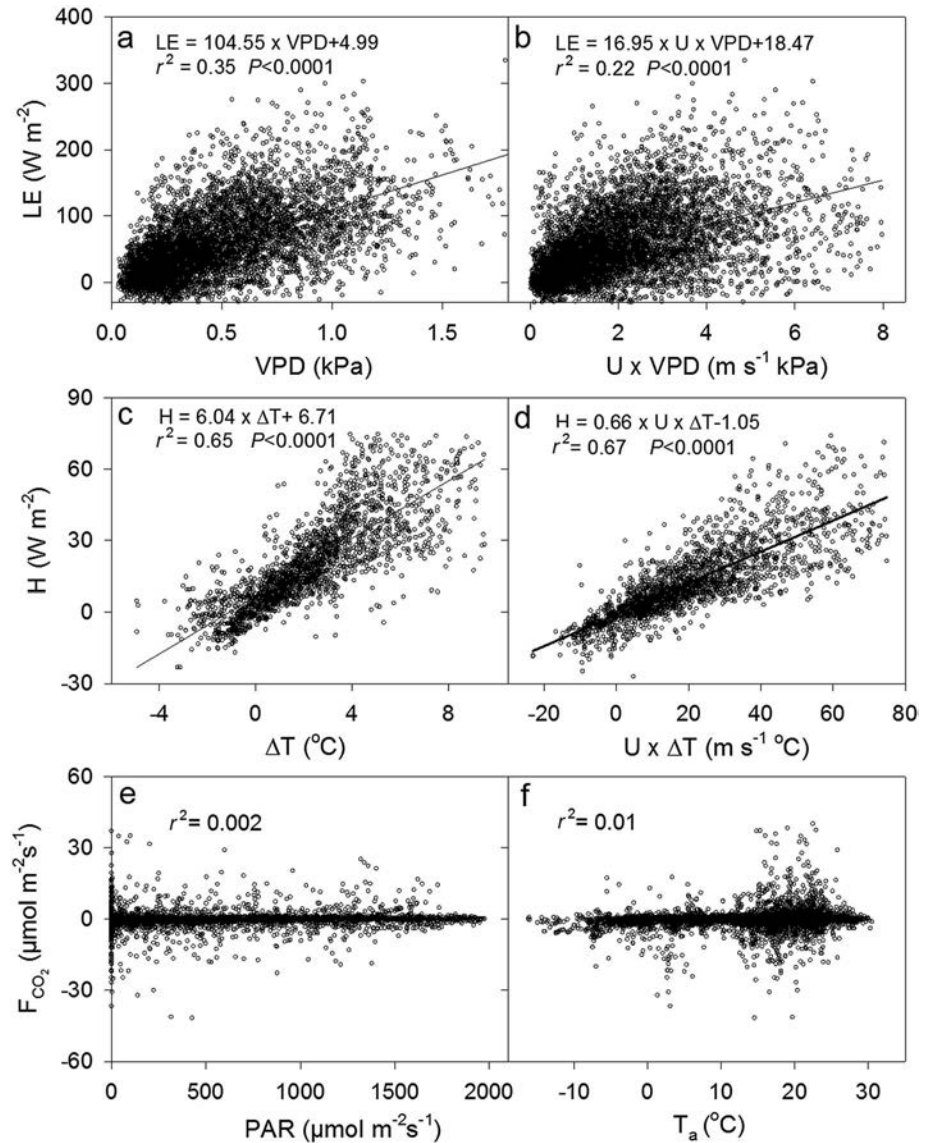


**Figure 9.** Relationships between latent heat flux ( $LE$ ) and (a) vapor pressure deficit ( $VPD$ ) and (b) product of  $U$  (wind speed) and  $VPD$ ; relationships between sensible heat flux ( $H$ ) and (c) the temperature difference  $\Delta T$  (surface water temperature at 0.20 m minus the air temperature at 16 m) and (d) product of  $U$  and  $\Delta T$ ; and relationships between  $CO_2$  flux ( $F_{CO_2}$ ) and (e) photosynthetically active radiation ( $PAR$ ) and (f) air temperature ( $T_a$ ) for Western Lake Erie. All quality-checked half hourly  $LE$  and  $CO_2$  data and all the quality-checked  $H$  data from 2011 to 2013 were used when water surface temperature was available. A linear fit with 95% confidence intervals, the correlation between the variables, and the linear model  $P$  value are shown in all plots.

was best explained by changes in  $VPD$  and  $U \times VPD$ . The  $VPD$  explained 35% of the variance in  $LE$  (Figure 9a), whereas  $U \times VPD$  was responsible for 22% (Figure 9b). Consequently, we attribute the spikes in  $LE$  (Figure 5) to strong wind activities, which deeply mixed the lake water and enhanced turbulent exchange [Blanken *et al.*, 2003; Rouse *et al.*, 2003]. We also found that the diurnal change in  $LE$  showed a greater correlation with  $U \times VPD$  ( $r^2 = 0.44$ ,  $P < 0.05$ ), rather than with  $R_n$  ( $r^2 = 0.23$ ,  $P < 0.05$ ; Figure S2). The reason may be due to an asynchronous effect (from Figure 5; higher  $LE$  was not at daytime but at nighttime) among different energy fluxes, resulting in a lower correlation with  $R_n$ . Driving forces for  $H$  were also evaluated. The temperature difference ( $\Delta T$ ) between the surface water temperature and the air temperature alone explained 65% of the variation in half hourly  $H$ , whereas  $U \times \Delta T$  explained 67% (Figures 9c and 9d), but neither  $H$  nor  $LE$  correlated markedly well with  $U$  at half hourly scale, which is consistent with Nordbo *et al.* [2011].

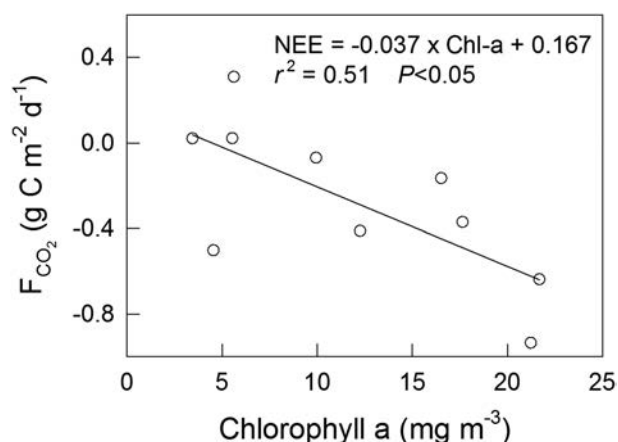


**Figure 10.** Monthly scale relationship between net ecosystem exchanges of CO<sub>2</sub> fluxes ( $F_{\text{CO}_2}$ ) with lake surface chlorophyll *a* content for Western Lake Erie. May–September data were used in 2012 and 2013.

A significantly negative correlation ( $P < 0.05$ ) was found between the  $F_{\text{CO}_2}$  and chlorophyll *a* on a monthly scale (Figure 10). Fifty percent of the variance in  $F_{\text{CO}_2}$  could be explained by the chlorophyll *a* content on a monthly scale. This result is consistent with those found in the terrestrial ecosystems, where fluxes over long temporal scales might reduce the instant positive/negative errors in flux measurements, and the true relationship may be detected between monthly  $F_{\text{CO}_2}$  and the controlling factors (i.e., PAR,  $T_a$ , RH, VPD, and  $U$ ). During the algal bloom periods, we also found strong correlations between the  $F_{\text{CO}_2}$  and the meteorological variables on a daily scale (Figure S3 in the supporting

information). The variable  $F_{\text{CO}_2}$  on a short time scale (Figure 6) suggests that multiple factors may determine  $F_{\text{CO}_2}$  dynamics, including biological and physical processes [Vesala *et al.*, 2006]. For example, the nighttime CO<sub>2</sub> uptake by the lake could be explained by the decrease in water temperature that increases CO<sub>2</sub> solubility in the water. Additionally, the allochthonous carbon could have originated from several anthropogenic sources, in addition to the chlorophyll *a* in the water. All point toward a stronger relationship between chlorophyll *a* and  $F_{\text{CO}_2}$  over a longer time scale than over a short time scale [Rantakari and Kortelainen, 2005; Linnaluoma, 2012]. Interestingly, we also found that the chlorophyll *a* and  $F_{\text{CO}_2}$  were negatively correlated with a time lag (weekly to monthly); i.e., peak chlorophyll *a* might not coincide with the smallest  $F_{\text{CO}_2}$  at a certain time scale, which increased the complexity to model the relationship between chlorophyll *a* and  $F_{\text{CO}_2}$ .

#### 4.4. Cross-Site Comparison of $F_{\text{CO}_2}$

Western Lake Erie acted as a small carbon sink in the summer and as a carbon source in the winter due to several reasons (Table 2). We hypothesized that the lake acted as carbon sink during the summer months because of the rich phytoplankton in this shallow waterbody; i.e., increased phytoplankton abundance leads to greater gross primary productivity and turns the lake to net autotrophy or from a net CO<sub>2</sub> source to a net CO<sub>2</sub> sink in the summer [Schindler *et al.*, 1997]. However, the net heterotrophic Western Lake Erie [Lavrentyev *et al.*, 2004] receives a massive amounts of organic materials laterally from its neighboring lands that is used by the bacterial community [Cole *et al.*, 2000]. Thus, the primary productivity of the lake may be offset. In fact, over the 2 year study period, Western Lake Erie acted as a CO<sub>2</sub> source annually and only during the period of cyanobacterial bloom (late summer and fall) did it act as a CO<sub>2</sub> sink. In addition, the pH was high and varied from 7.8 in early spring to 8.8 during the cyanobacterial blooms period for late July and early August in both years, meaning that only a small fraction of dissolved inorganic carbon was in the form of CO<sub>2</sub> [Cole *et al.*, 2007]. This might be another reason why Western Lake Erie acted as a carbon sink in the summer. With the cyanobacterial bloom disappearing, the lake turned to a net CO<sub>2</sub> source in other seasons in both years. Our observations were consistent with the model study that the lake acts as a CO<sub>2</sub> sink in summer and as a source during winter and spring [Bennington *et al.*, 2012]. The vigorous phytoplankton growth (Figure 4), accompanied with a bit higher carbon absorption (Table 2), might correlate with more rain (Table 1) that brings more phosphorous into the lake in Year 2. Our results also support that the northern lakes generally acted as sources of CO<sub>2</sub> on an annual scale [Cole *et al.*, 1994; Jonsson *et al.*, 2008; Huotari *et al.*, 2011].

The present study is the first long-term  $F_{\text{CO}_2}$  field campaign conducted in Lake Erie with the EC technique. There exist only a few published short/long-term CO<sub>2</sub> studies with EC measurements on lakes available for comparison (Table 3). Anderson *et al.* [1999] measured fluxes from  $-0.17$  to  $2.7 \mu\text{mol m}^{-2} \text{s}^{-1}$  during a couple of days directly following an ice melt in Williams Lake in Minnesota. Vesala *et al.* [2006] found that a boreal lake acted as a source of carbon, with CO<sub>2</sub> fluxes varying from  $0.2 \mu\text{mol m}^{-2} \text{s}^{-1}$  in May to  $0.4 \mu\text{mol m}^{-2} \text{s}^{-1}$  in August.

**Table 3.** Comparative Ecosystem Characteristics of Our Eddy Covariance Measurements With Those From Other Lakes<sup>a</sup>

Lake	Latitude	Area (km <sup>2</sup> )	Depth (m)	Flux Measurement Period	Offshore/ Fetch(m)	Minimum F <sub>CO<sub>2</sub></sub>	Maximum F <sub>CO<sub>2</sub></sub>	Daily F <sub>CO<sub>2</sub></sub>	Annual F <sub>CO<sub>2</sub></sub>	Source
Williams Lake, Minnesota, USA	46.57°N	0.3409	5.2	1992–1994, 5 weeks	300	-0.17 (Summer)	2.70	na	na	Anderson et al. [1999]
Toolik Lake, Alaska, USA	68.37°N	1.5	7.0	1994–1995, 7 days	200	-0.42	1.25	0.11	na	Eugster et al. [2003]
Valkea-Kotinen Lake, Finland <sup>b</sup>	61.14°N	0.041	2.5	Apr–Nov 2003	35	-0.04 (July)	0.39	na	na	Vesala et al. [2006]
				Apr 2005 to Oct 2006	35	na	na	na	110	Huotari et al. [2009]
				2003–2007	35	na	na	0.21	77	Huotari et al. [2011]
Lake Merasjarv, northern Sweden	67.55°N	3.8	5.1	17 Jun to 15 Oct 2005	350	na	na	0.20	na	Jonsson et al. [2008]
Amazon River, northern Brazil	2.96°N	450	45	19–22 Nov 2011	edge	0.05	2.2	na	na	Polsenaere et al. [2013]
Lake Tjörnaren, Sweden	60.15°N	38	1.3	2011	1,000	na	na	0.10	na	Podgrajsek et al. [2014a]
				Jan–Sept 2012	1,000	na	3.60	0.57	na	Podgrajsek et al. [2014b]
				Sept 2010–Sept 2012	1,000	-0.78	1.62	0.18	63	This study
				Oct 2011 to Sept 2013 <sup>c</sup>	12,000	-0.06	1.09	0.17	63	
				Oct 2011 to Sept 2012 (Year 1)	12,000	-0.17	1.15	0.21	76	
				Oct 2012 to Sept 2013 (Year 2)	12,000	-0.06	1.28	0.14	50	
				Jan 2012 to Dec 2012	12,000	-0.01	1.19	0.22	79	

<sup>a</sup>CO<sub>2</sub> flux (F<sub>CO<sub>2</sub></sub>). Units are μmol CO<sub>2</sub> m<sup>-2</sup> s<sup>-1</sup> for minimum and maximum F<sub>CO<sub>2</sub></sub>, and g C m<sup>-2</sup> yr<sup>-1</sup> for annual F<sub>CO<sub>2</sub></sub>, na, data not available.

<sup>b</sup>Across entire series of measurements.

<sup>c</sup>Note that the lake is 500 m elongated in its shape.

Eugster et al. [2003] reported summertime fluxes of -0.42 to 1.25 μmol m<sup>-2</sup> s<sup>-1</sup> over Toolik Lake in Alaska that were comparable to ours as -0.17 to 1.28 μmol m<sup>-2</sup> s<sup>-1</sup>. Clearly, the CO<sub>2</sub> exchange between the lake surface and the atmosphere varies among lakes and over time. Our continuous measurements and our cross-site collaborations with others are needed to reach a sound conclusion.

On average, the Western Lake Erie site released 63 g C m<sup>-2</sup> yr<sup>-1</sup> over the 2 years. Our results resemble those from Valkea-Kotinen Lake in Finland, where 68–97 g C m<sup>-2</sup> yr<sup>-1</sup> was reported by Huotari et al. [2011]. Our results also were greater than a corn cropland that sequestered ~60 g C m<sup>-2</sup> yr<sup>-1</sup> located near our watershed [Zenone et al., 2013] and much less than the uptake of an adjacent forest with 340 g C m<sup>-2</sup> yr<sup>-1</sup> [Xie et al., 2014]. Considering the size area of Lake Erie, its overall contribution will be much greater. Scaling our results across the entire Western Lake Erie Basin, its estimated release is 3.3 × 10<sup>5</sup> t C/yr. Based on the relative spatial coverage of croplands (~70%) and forests (~7%) in the region [Chu et al., 2014a], and with about 10 times watershed area of the basin, this carbon loss from the Western Lake Erie is equivalent to one fourth of the carbon sink of natural forests or one fifth of the croplands in the Western Lake Erie Basin watershed.

### 5. Conclusions

We report the changes in latent and sensible heat and CO<sub>2</sub> fluxes using the micrometeorological eddy covariance technique from 2011 to 2013 in Western Lake Erie. We found that the Western Lake Erie Basin acted as a net carbon source over the 2 year study period but as a small carbon sink during the summer in both years. A significantly strong correlation was found between the carbon flux and chlorophyll *a* on a monthly scale. The amount of yearly released carbon from Western Lake Erie was equivalent to one fourth of the carbon sequestered by adjacent forests in the watershed. Our results also showed that the evaporation for Western Lake Erie returns approximately 90% of annual rainfall to the atmosphere. These results indicate that natural inland waters

constitute an integral part of the regional carbon and water cycling and therefore must be taken into account during balance calculations and when considering the regional macrosystem strength in modeling carbon and water cycles.

#### Acknowledgments

We thank Michael Deal, Yahn-Jauh Su, Cody Kish, Butch Berger, Andrew McClure, Brenda Snyder, and others from the City of Toledo Division of Water Treatment for building and maintaining the site infrastructure and assisting in the data collection and management. Our site was supported by NOAA Great Lakes Environmental Research Laboratory, for which we especially thank Steve Ruberg for his help. We also thank Gabriela Shirkey for her language editing throughout the manuscript. This study was supported by the Field Station and Marine Labs Program of the National Science Foundation (NSF1034791), the NASA-NEWS Program (NN-H-04-Z-YS-005-N), and the USCCC. Part of the data for this paper is available at our project website: [http://lees.geo.msu.edu/research/sensor\\_net/index.html](http://lees.geo.msu.edu/research/sensor_net/index.html).

#### References

- Alavi, N., J. S. Warland, and A. A. Berg (2006), Filling gaps in evapotranspiration measurements for water budget studies: Evaluation of a Kalman filtering approach, *Agric. For. Meteorol.*, *141*(1), 57–66, doi:10.1016/j.agrformet.2006.09.011.
- Allen, R. G., L. S. Pereira, D. Raes, and M. Smith (1998), FAO irrigation and drainage paper, No. 56, Crop evapotranspiration, Guidelines for computing crop water requirements. [Available at <http://www.fao.org/docrep/x0490e/x0490e00.htm>.]
- Anderson, D. E., R. G. Striegl, D. I. Stannard, C. M. Michmerhuizen, T. A. McConnaughey, and J. W. LaBaugh (1999), Estimating lake-atmosphere CO<sub>2</sub> exchange, *Limnol. Oceanogr.*, *44*(4), 988–1001.
- Atilla, N., G. A. McKinley, V. Bennington, M. Baehr, N. Urban, M. DeGrandpre, A. R. Desai, and C. Wu (2011), Observed variability of Lake Superior pCO<sub>2</sub>, *Limnol. Oceanogr.*, *56*(3), 775–786, doi:10.4319/lo.2011.56.3.0775.
- Aurela, M., T. Laurila, and J. P. Tuovinen (2002), Annual CO<sub>2</sub> balance of a subarctic fen in northern Europe: Importance of the wintertime efflux, *J. Geophys. Res.*, *107*(D21), 4607, doi:10.1029/2002JD002055.
- Baldocchi, D., B. E. Law, and P. M. Anthoni (2000), On measuring and modeling energy fluxes above the floor of a homogeneous and heterogeneous conifer forest, *Agric. For. Meteorol.*, *102*, 187–206.
- Baldocchi, D., et al. (2001), FLUXNET: A new tool to study the temporal and spatial variability of ecosystem-scale carbon dioxide, water vapor, and energy flux densities, *Bull. Am. Meteorol. Soc.*, *82*(11), 2415–2434, doi:10.1175/1520-0477(2001)082<2415:fantts>2.3.co;2.
- Bennington, V., G. A. McKinley, N. R. Urban, and C. P. McDonald (2012), Can spatial heterogeneity explain the perceived imbalance in Lake Superior's carbon budget? A model study, *J. Geophys. Res.*, *117*, G03020, doi:10.1029/2011JG001895.
- Blanken, P. D., W. R. Rouse, A. D. Culf, C. Spence, L. D. Boudreau, J. N. Jasper, B. Kochtubajda, W. M. Schertzer, P. Marsh, and D. Versegny (2000), Eddy covariance measurements of evaporation from Great Slave Lake, Northwest Territories, Canada, *Water Resour. Res.*, *36*(4), 1069–1077, doi:10.1029/1999WR900338.
- Blanken, P. D., W. R. Rouse, and W. M. Schertzer (2003), Enhancement of evaporation from a large northern lake by the entrainment of warm, dry air, *J. Hydrometeorol.*, *4*(4), 680–693, doi:10.1175/1525-7541(2003)004<0680:eoefal>2.0.co;2.
- Blanken, P. D., C. Spence, N. Hedstrom, and J. D. Lenters (2011), Evaporation from Lake Superior: 1. Physical controls and processes, *J. Great Lakes Res.*, *37*(4), 707–716, doi:10.1016/j.jglr.2011.08.009.
- Bridgeman, T. B., J. D. Chaffin, and J. E. Filbrun (2013), A novel method for tracking Western Lake Erie Microcystis blooms, 2002–2011, *J. Great Lakes Res.*, *39*(1), 83–89, doi:10.1016/j.jglr.2012.11.004.
- Chen, J., J. F. Franklin, and T. A. Spies (1993), An empirical-model for predicting diurnal air-temperature gradients from edge into old-growth Douglas-fir forest, *Ecol. Modell.*, *67*(2–4), 179–198, doi:10.1016/0304-3800(93)90004-c.
- Chen, J., K. T. Paw U, S. L. Ustin, T. H. Suchanek, B. J. Bond, K. D. Brososke, and M. Falk (2004), Net ecosystem exchanges of carbon, water, and energy in young and old-growth Douglas-fir forests, *Ecosystems*, *7*(5), 534–544, doi:10.1007/s10021-004-0143-6.
- Chu, H., N. Liang, C. Lai, C. Wu, S. Chang, and Y. Hsia (2013), Topographic effects on CO<sub>2</sub> flux measurements at the Chi-Lan Mountain forest, *Taiwan J. For. Sci.*, *28*, 1–16. [Available at <http://www.airitilibrary.com/Publication/alDetailedMesh?docid=10264469-201303-201305200008-201305200008-1-16>.]
- Chu, H., J. Chen, J. F. Gottgens, Z. Ouyang, R. John, K. Czajkowski, and R. Becker (2014a), Net ecosystem CH<sub>4</sub> and CO<sub>2</sub> exchanges in a Lake Erie coastal marsh and a nearby cropland, *J. Geophys. Res. Biogeosci.*, *119*, 722–740, doi:10.1002/2013JG002520.
- Chu, H., J. F. Gottgens, J. Chen, G. Sun, A. R. Desai, Z. Ouyang, C. Shao, and K. Czajkowski (2014b), Climatic variability, hydrologic anomaly, and methane emission can turn productive freshwater marshes into net carbon sources, *Global Change Biol.*, *21*(3), 1165–1181, doi:10.1111/gcb.12760.
- Cole, J. J., and N. F. Caraco (1998), Atmospheric exchange of carbon dioxide in a low-wind oligotrophic lake measured by the addition of SF<sub>6</sub>, *Limnol. Oceanogr.*, *43*(4), 647–656, doi:10.4319/lo.1998.43.4.0647.
- Cole, J. J., N. F. Caraco, G. W. Kling, and T. K. Kratz (1994), Carbon-dioxide supersaturation in the surface waters of lakes, *Science*, *265*(5178), 1568–1570, doi:10.1126/science.265.5178.1568.
- Cole, J. J., M. L. Pace, S. R. Carpenter, and J. F. Kitchell (2000), Persistence of net heterotrophy in lakes during nutrient addition and food web manipulations, *Limnol. Oceanogr.*, *45*(8), 1718–1730.
- Cole, J. J., et al. (2007), Plumbing the global carbon cycle: Integrating inland waters into the terrestrial carbon budget, *Ecosystems*, *10*(1), 171–184, doi:10.1007/s10021-006-9013-8.
- Coyne, P. I., and J. J. Kelley (1974), Carbon-dioxide partial pressures in arctic surface waters, *Limnol. Oceanogr.*, *19*(6), 928–938.
- Crusius, J., and R. Wanninkhof (2003), Gas transfer velocities measured at low wind speed over a lake, *Limnol. Oceanogr.*, *48*(3), 1010–1017, doi:10.4319/lo.2003.48.3.1010.
- Eugster, W., G. Kling, T. Jonas, J. P. McFadden, A. Wuest, S. MacIntyre, and F. S. Chapin (2003), CO<sub>2</sub> exchange between air and water in an Arctic Alaskan and midlatitude Swiss lake: Importance of convective mixing, *J. Geophys. Res.*, *108*(D12), 4362, doi:10.1029/2002JD002653.
- Falge, E., et al. (2001a), Gap filling strategies for long term energy flux data sets, *Agric. For. Meteorol.*, *107*(1), 71–77.
- Falge, E., D. Baldocchi, R. Olson, P. Anthoni, M. Aubinet, C. Bernhofer, G. Burba, R. Ceulemans, R. Clement, and H. Dolman (2001b), Gap filling strategies for defensible annual sums of net ecosystem exchange, *Agric. For. Meteorol.*, *107*(1), 43–69.
- Foken, T., and B. Wichura (1996), Tools for quality assessment of surface-based flux measurements, *Agric. For. Meteorol.*, *78*(1–2), 83–105, doi:10.1016/0168-1923(95)02248-1.
- Gronewold, A. D., V. Fortin, B. Lofgren, A. Clites, C. A. Stow, and F. Quinn (2013), Coasts, water levels, and climate change: A Great Lakes perspective, *Clim. Change*, *120*(4), 697–711, doi:10.1007/s10584-013-0840-2.
- Guildford, S. J., R. E. Hecky, R. E. H. Smith, W. D. Taylor, M. N. Charlton, L. Barlow-Busch, and R. L. North (2005), Phytoplankton nutrient status in Lake Erie in 1997, *J. Great Lakes Res.*, *31*, 72–88.
- Hanson, P. C., A. I. Pollard, D. L. Bade, K. Predick, S. R. Carpenter, and J. A. Foley (2004), A model of carbon evasion and sedimentation in temperate lakes, *Global Change Biol.*, *10*(8), 1285–1298, doi:10.1111/j.1365-2486.2004.00805.x.
- Heikkinen, J. E. P., T. Virtanen, J. T. Huttunen, V. Elsakov, and P. J. Martikainen (2004), Carbon balance in East European tundra, *Global Biogeochem. Cycles*, *18*, GB1023, doi:10.1029/2003GB002054.
- Herdendorf, C. E., and M. E. Monaco (1988), Physical and chemical limnology of the island region of Lake Erie, in *The Biogeography of the Island Region of Western Lake Erie*, edited by J. F. Downhower, chap. 4, pp. 30–42, The Ohio State Univ. Press, Columbus, Ohio.

- Huotari, J., A. Ojala, E. Peltomaa, J. Pumpanen, P. Hari, and T. Vesala (2009), Temporal variations in surface water CO<sub>2</sub> concentration in a boreal humic lake based on high-frequency measurements, *Boreal Environ. Res.*, *14*, 48–60. [Available at <http://www.borenav.net/BER/pdfs/ber14/ber14A-048.pdf>.]
- Huotari, J., A. Ojala, E. Peltomaa, A. Nordbo, S. Launiainen, J. Pumpanen, T. Rasilo, P. Hari, and T. Vesala (2011), Long-term direct CO<sub>2</sub> flux measurements over a boreal lake: Five years of eddy covariance data, *Geophys. Res. Lett.*, *38*, L18401, doi:10.1029/2011GL048753.
- Ikawa, H., I. Faloon, J. Kochendorfer, K. T. Paw U, and W. C. Oechel (2013), Air–sea exchange of CO<sub>2</sub> at a Northern California coastal site along the California Current upwelling system, *Biogeosciences*, *10*(7), 4419–4432, doi:10.5194/bg-10-4419-2013.
- Inskeep, W. P., and P. R. Bloom (1985), Extinction coefficients of chlorophyll-*a* and chlorophyll-*b* in N, N-dimethylformamide and 80% acetone, *Plant Physiol.*, *77*(2), 483–485, doi:10.1104/pp.77.2.483.
- Jonsson, A., J. Aberg, A. Lindroth, and M. Jansson (2008), Gas transfer rate and CO<sub>2</sub> flux between an unproductive lake and the atmosphere in northern Sweden, *J. Geophys. Res.*, *113*, G04006, doi:10.1029/2008JG000688.
- Kormann, R., and F. Meixner (2001), An analytical footprint model for non-neutral stratification, *Boundary Layer Meteorol.*, *99*(2), 207–224, doi:10.1023/a:1018991015119.
- Kortelainen, P., M. Rantakari, J. T. Huttunen, T. Mattsson, J. Alm, S. Juutinen, T. Larmola, J. Silvola, and P. J. Martikainen (2006), Sediment respiration and lake trophic state are important predictors of large CO<sub>2</sub> evasion from small boreal lakes, *Global Change Biol.*, *12*(8), 1554–1567, doi:10.1111/j.1365-2486.2006.01167.x.
- Lavrentyev, P. J., M. J. McCarthy, D. M. Klarer, F. Jochem, and W. S. Gardner (2004), Estuarine microbial food web patterns in a Lake Erie coastal wetland, *Microb. Ecol.*, *48*(4), 567–577, doi:10.1007/s00248-004-0250-0.
- LI-COR (2004), *LI-7500 Open Path CO<sub>2</sub> Analyzer Instruction Manual*, LI-COR, Inc. Biosciences, Lincoln, Nebr.
- Linnaluoma, J. (2012), Factors controlling carbon gas fluxes in boreal lakes, Academic dissertation in Environmental Ecology, Dep. of Environ. Sci., Aquatic Sci., pp. 1–73, Univ. of Helsinki, Lahti, Finland.
- Liu, H. P., Y. Zhang, S. Liu, H. Jiang, L. Sheng, and Q. L. Williams (2009), Eddy covariance measurements of surface energy budget and evaporation in a cool season over southern open water in Mississippi, *J. Geophys. Res.*, *114*, D04110, doi:10.1029/2008JD010891.
- Liu, H. P., Q. Y. Zhang, and G. Dowler (2012), Environmental controls on the surface energy budget over a large southern inland water in the united states: An analysis of one-year eddy covariance flux data, *J. Hydrometeorol.*, *13*(6), 1893–1910, doi:10.1175/jhm-d-12-020.1.
- Lofgren, B. M. (1997), Simulated effects of idealized Laurentian Great Lakes on regional and large-scale climate, *J. Clim.*, *10*(11), 2847–2858, doi:10.1175/1520-0442(1997)010<2847:seoilg>2.0.co;2.
- Lofgren, B. M., F. H. Quinn, A. H. Clites, R. A. Assel, A. J. Eberhardt, and C. L. Luukkonen (2002), Evaluation of potential impacts on Great Lakes water resources based on climate scenarios of two GCMs, *J. Great Lakes Res.*, *28*(4), 537–554.
- Long, Z., W. Perrie, J. Gyakum, D. Caya, and R. Laprise (2007), Northern lake impacts on local seasonal climate, *J. Hydrometeorol.*, *8*(4), 881–896, doi:10.1175/jhm591.1.
- Michalak, A. M., et al. (2013), Record-setting algal bloom in Lake Erie caused by agricultural and meteorological trends consistent with expected future conditions, *Proc. Natl. Acad. Sci. U.S.A.*, *110*(16), 6448–6452, doi:10.1073/pnas.1216006110.
- Moncrieff, J., R. Clement, J. Finnigan, and T. Meyers (2004), Averaging, detrending, and filtering of eddy covariance time series, in *Handbook of Micrometeorology: A Guide for Surface Flux Measurement and Analysis*, edited by X. Lee, W. Massman, and B. Law, pp. 7–32, Kluwer Acad., Dordrecht, Netherlands.
- Nordbo, A., S. Launiainen, I. Mammarella, M. Lepparanta, J. Huotari, A. Ojala, and T. Vesala (2011), Long-term energy flux measurements and energy balance over a small boreal lake using eddy covariance technique, *J. Geophys. Res.*, *116*, D02119, doi:10.1029/2010JD014542.
- O'Donnell, D. M., S. W. Effler, C. M. Strait, and G. A. Leshkevich (2010), Optical characterizations and pursuit of optical closure for the Western Basin of Lake Erie through in situ measurements, *J. Great Lakes Res.*, *36*(4), 736–746, doi:10.1016/j.jglr.2010.08.009.
- Oki, T., and S. Kanae (2006), Global hydrological cycles and world water resources, *Science*, *313*(5790), 1068–1072, doi:10.1126/science.1128845.
- O'Reilly, J. E. (2000), Ocean color chlorophyll *a* algorithms for SeaWiFS, OC2 and OC4: Version 4, in *SeaWiFS Postlaunch Calibration and Validation Analyses, Part 3. NASA Tech. Memo 2000–206892*, vol. 11, edited by S. B. Hooker and E. R. Firestone, pp. 9–23, NASA Goddard Space Flight Center, Greenbelt, Md.
- Podgrajsek, E., E. Sahlée, D. Bastviken, J. Holst, A. Lindroth, L. Tranvik, and A. Rutgersson (2014a), Comparison of floating chamber and eddy covariance measurements of lake greenhouse gas fluxes, *Biogeosciences*, *11*(15), 4225–4233, doi:10.5194/bg-11-4225-2014.
- Podgrajsek, E., E. Sahlée, and A. Rutgersson (2014b), Diel cycle of lake-air CO<sub>2</sub> flux from a shallow lake and the impact of watershed convection on the transfer velocity, *J. Geophys. Res. Biogeosci.*, *120*, 29–38, doi:10.1002/2014JG002781.
- Polsenaere, P., J. Deborde, G. Detandt, L. O. Vidal, M. A. P. Perez, V. Marieu, and G. Abril (2013), Thermal enhancement of gas transfer velocity of CO<sub>2</sub> in an Amazon floodplain lake revealed by eddy covariance measurements, *Geophys. Res. Lett.*, *40*, 1734–1740, doi:10.1002/grl.50291.
- Rantakari, M., and P. Kortelainen (2005), Interannual variation and climatic regulation of the CO<sub>2</sub> emission from large boreal lakes, *Global Change Biol.*, *11*(8), 1368–1380, doi:10.1111/j.1365-2486.2005.00982.x.
- Reichstein, M., et al. (2005), On the separation of net ecosystem exchange into assimilation and ecosystem respiration: Review and improved algorithm, *Global Change Biol.*, *11*(9), 1424–1439, doi:10.1111/j.1365-2486.2005.001002.x.
- Richey, J. E., J. M. Melack, A. K. Aufdenkampe, V. M. Ballester, and L. L. Hess (2002), Outgassing from Amazonian rivers and wetlands as a large tropical source of atmospheric CO<sub>2</sub>, *Nature*, *416*(6881), 617–620, doi:10.1038/416617a.
- Rouse, W. R., C. M. Oswald, J. Binyamin, P. D. Blanken, W. M. Schertzer, and C. Spence (2003), Interannual and seasonal variability of the surface energy balance and temperature of central Great Slave Lake, *J. Hydrometeorol.*, *4*(4), 720–730, doi:10.1175/1525-7541(2003)004<0720:iasvot>2.0.co;2.
- Rouse, W. R., C. J. Oswald, J. Binyamin, C. R. Spence, W. M. Schertzer, P. D. Blanken, N. Bussieres, and C. R. Duguay (2005), The role of northern lakes in a regional energy balance, *J. Hydrometeorol.*, *6*(3), 291–305, doi:10.1175/jhm421.1.
- Rudorff, C. M., J. M. Melack, S. MacIntyre, C. C. F. Barbosa, and E. M. L. M. Novo (2011), Seasonal and spatial variability of CO<sub>2</sub> emission from a large floodplain lake in the lower Amazon, *J. Geophys. Res.*, *116*, G04007, doi:10.1029/2011JG001699.
- Schindler, D. E., S. R. Carpenter, J. J. Cole, J. F. Kitchell, and M. L. Pace (1997), Influence of food web structure on carbon exchange between lakes and the atmosphere, *Science*, *277*(5323), 248–251, doi:10.1126/science.277.5323.248.
- Shao, C., J. Chen, L. Li, W. Xu, S. Chen, T. Gwen, J. Xu, and W. Zhang (2008), Spatial variability in soil heat flux at three Inner Mongolia steppe ecosystems, *Agric. For. Meteorol.*, *148*(10), 1433–1443, doi:10.1016/j.agrformet.2008.04.008.
- Vesala, T., J. Huotari, U. Rannik, T. Suni, S. Smolander, A. Sogachev, S. Launiainen, and A. Ojala (2006), Eddy covariance measurements of carbon exchange and latent and sensible heat fluxes over a boreal lake for a full open-water period, *J. Geophys. Res.*, *111*, D11101, doi:10.1029/2005JD006365.

- Wilczak, J. M., S. P. Oncley, and S. A. Stage (2001), Sonic anemometer tilt correction algorithms, *Boundary Layer Meteorol.*, *99*(1), 127–150, doi:10.1023/a:1018966204465.
- Xiao, J., et al. (2013), Carbon fluxes, evapotranspiration, and water use efficiency of terrestrial ecosystems in China, *Agric. For. Meteorol.*, *182–183*, 76–90, doi:10.1016/j.agrformet.2013.08.007.
- Xie, J., J. Chen, G. Sun, H. Chu, A. Noormets, Z. Ouyang, R. John, S. Wan, and W. Guan (2014), Long-term variability and environmental control of the carbon cycle in an oak-dominated temperate forest, *For. Ecol. Manage.*, *313*, 319–328, doi:10.1016/j.foreco.2013.10.032.
- Zenone, T., I. Gelfand, J. Chen, S. K. Hamilton, and G. P. Robertson (2013), From set-aside grassland to annual and perennial cellulosic biofuel crops: Effects of land use change on carbon balance, *Agric. For. Meteorol.*, *182–183*, 1–12, doi:10.1016/j.agrformet.2013.07.015.